Topological boundaries between helical domains as a nucleation source of skyrmions in the bulk cubic helimagnet Cu2OSeO3

Leonov, A. O.; Pappas, C.

DOI
10.1103/PhysRevResearch.4.043137

Publication date
2022

Document Version
Final published version

Published in
Physical Review Research

Topological boundaries between helical domains as a nucleation source of skyrmions in the bulk cubic helimagnet Cu_2OSeO_3

A. O. Leonov[1,2,3,*] and C. Pappas[4,†]

[1]*Department of Chemistry, Faculty of Science, Hiroshima University Kagamiyama, Higashi Hiroshima, Hiroshima 739-8526, Japan*
[2]*IFW Dresden, IFW Institute for Theoretical Solid State Physics, Postfach 270016, D-01171 Dresden, Germany*
[3]*International Institute for Sustainability with Knotted Chiral Meta Matter, Kagamiyama, Higashi Hiroshima, Hiroshima 739-8526, Japan*
[4]*Faculty of Applied Sciences, Delft University of Technology, Mekelweg 15, 2629JB Delft, The Netherlands*

(Received 2 June 2022; revised 2 September 2022; accepted 6 October 2022; published 28 November 2022)

Cu_2OSeO_3 represents a unique example in the family of B20 cubic helimagnets with a tilted spiral and a low-temperature skyrmion phase arising for magnetic fields applied along the easy crystallographic ⟨100⟩ axes. Although the stabilization mechanism of these phases can be accounted for by cubic magnetic anisotropy, the skyrmion nucleation process is still an open question, since the stability region of the skyrmion phase displays strongly hysteretic behavior with different phase boundaries for increasing and decreasing magnetic fields. Here, we address this important point using micromagnetic simulations and come to the conclusion that skyrmion nucleation is underpinned by the reorientation of spiral domains occurring near the critical magnetic fields of the phase diagrams: H_{C1}, the critical field of the transition between the helical and conical/tiled spiral phase, and H_{C2}, the critical field between the conical/tiled spiral and the homogenous phase. By studying a wide variety of cases we show that domain walls may have a 3D structure. Moreover, they can carry a finite topological charge stemming from half-skyrmions (merons) also permitting along-the-field and perpendicular-to-the-field orientation. Thus, domain walls may be envisioned as nucleation source of skyrmions that can form thermodynamically stable and metastable lattices as well as skyrmion networks with misaligned skyrmion tubes. The results of numerical simulations are discussed in view of recent experimental data on chiral magnets, in particular, for the bulk cubic helimagnet Cu_2OSeO_3.

DOI: 10.1103/PhysRevResearch.4.043137

I. INTRODUCTION

Chiral magnetic skyrmions—topological defects with a complex noncoplanar magnetic structure, combining rotational and longitudinal modulations of the magnetization, [1,2]—were first experimentally identified in bulk cubic helimagnets such as the itinerant magnets, MnSi [3] and FeGe [4], and the Mott insulator, Cu_2OSeO_3 [5]. In these systems, skyrmions form hexagonal lattices in a small pocket of the temperature-magnetic field (T-H) phase diagrams just below the transition temperature T_C, the so-called A-phase. For these "high-temperature" (HT) magnetic skyrmions, the "softening" of the magnetization modulus **m** has dramatic consequences [4,6–8]. First, this leads to a remarkable confinement effect near the ordering temperature, where skyrmions exist only as bound states that attract each other and form skyrmion lattices (SkL) by an unusual *instability-type nucleation transition* given that the creation of skyrmions as stable units and their condensation into different extended textures occurs simultaneously [6–8]. As skyrmions retain their size and axisymmetric shape, there is a full spectrum of lattice modes up to the transition, in contrary to ordinary instability type transitions where the amplitude of one fundamental mode acts as parameter of the transition [9]. Second, the difference between the energies of the hexagonal skyrmion lattice $W_{\rm SkL}$ and the conical phase $W_{\rm cone}$, calculated for the isotropic Dzyaloshinskii model (2), $\Delta W_{\rm min} = W_{\rm SkL} - W_{\rm cone}$, has minima along a curve $\xi(T)$ exactly for those magnetic fields that stabilize the A-phase [7,8]. Consequently, weak additional terms may modify the energetic landscape and eventually favor the SkL in the A-phase pocket. Such weak additional effects can therefore provide mechanisms for complex and unconventional magnetic phase diagrams and may stabilize exotic phases such as a square staggered lattice of half-skyrmions [10,11].

For cubic helimagnets, the isotropic energy density [introduced later in Eq. (2)] is usually supplemented by exchange and cubic anisotropic contributions [11,12],

$$\Phi_a = b_{\rm ea}(T)\sum_i (\partial m_i/\partial x_i)^2 + k_c(T)\sum_i m_i^4, \qquad (1)$$

where $b_{\rm ea}$ and k_c are reduced anisotropy constants, which are in general temperature-dependent. The theoretical explanation of the anisotropy-induced SkL stability (1) is mainly based on the effect imposed on one-dimensional spiral states. In fact, the ideal magnetization rotation in the conical phase, the main competitor of skyrmions surrounding the A-phase

*leonov@hiroshima-u.ac.jp
†c.pappas@tudelft.nl

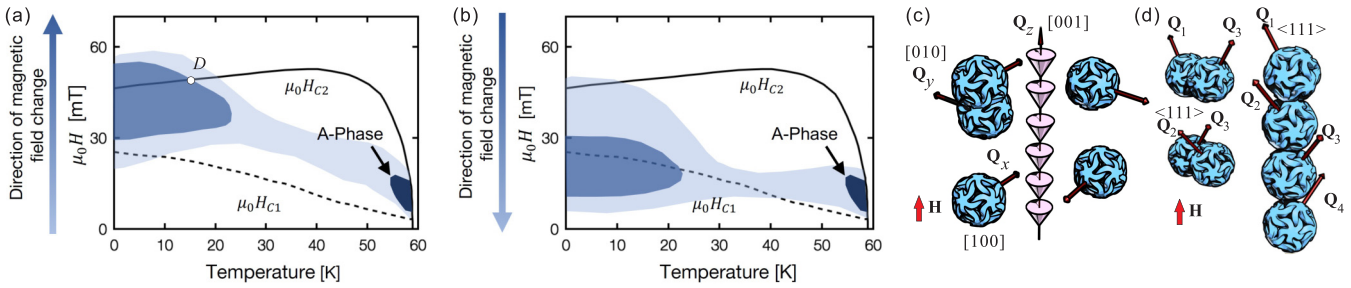

FIG. 1. Experimental phase diagrams indicating the extent and intensity of skyrmionic scattering after zero field cooling (ZFC) for $\mathbf{H}||\mathbf{k}_i|||[001]$. The measurements were performed upon increasing the magnetic field (a) and decreasing the magnetic field (b). Deep dark blue stands for the high-temperature A-phase; dark blue—for the low-temperature SkL; and light blue—for the weak scattering that surrounds both the LT and HT skyrmion pockets and connects them. (c) Schematics showing coexisting helical domains with mutually orthogonal propagation directions (shown as blue balls). In an applied magnetic field, only the conical phase constitutes the energy minimum, whereas other spirals turn metastable. (d) Schematics showing coexisting domains of an oblique spiral tilting toward ⟨111⟩ directions.

region [Fig. 1(a) and 1(b)], can be impaired by the easy and hard anisotropy axes for specific directions of the magnetic field. Through this mechanism, skyrmions gain stability as they are more resilient to anisotropy-induced deformations, due to their two-dimensional nature [12].

In contrast to the A-phase skyrmions, which exist in the narrow temperature interval of the A-phase ($T_{cf} < T < T_C$) (where T_{cf} is a characteristic crossover temperature introduced in Refs. [7,8]) and are characterized by the mentioned coupling between rotational and longitudinal modes, chiral modulated textures are composed of only rotational modes (and are called henceforth regular modulations) over a much broader temperature range from 0 to T_{cf}. Recently, such a regular "low-temperature" (LT) skyrmion phase was shown to occupy a large area of the magnetic phase diagram in a bulk helimagnet Cu_2OSeO_3 and extend from the lowest temperatures up to the A-phase [Figs. 1(a) and 1(b)] [13,14]. This LT skyrmion phase appears for a magnetic field **H** applied along the easy magnetization ⟨100⟩ directions [13,14] and its stability was attributed to the cubic anisotropy, through the same mechanism that could also stabilize HT-skyrmions. Furthermore, in the same sample and for the same direction of the magnetic field, the competition between cubic and exchange anisotropies (1) also stabilizes a tilted spiral phase [13,15].

The nucleation mechanism of stable LT skyrmions, however, is still an open question. Theoretically, one may approach it following a classification introduced by DeGennes [9] for (continuous) transitions into incommensurate modulated phases. According to DeGennes, the conical state is stable locally, but it becomes unstable with respect to certain distortions of large amplitude such as skyrmions. In this scenario, defect-free isolated skyrmions would be formed, e.g., via torons [16,17], which are spatially localized three-dimensional particles composed of a skyrmion filament of finite length cupped by two point defects. And in fact cubic anisotropy k_c facilitates toron elongation since it makes the skyrmion cores energetically favourable with respect to the surrounding parental state. And indeed Ref. [14] reported that skyrmions are surprisingly resilient to high magnetic fields. The memory of skyrmion lattice states was shown to persist in the field polarized state possibly in the form of torons, even when the skyrmion lattice signal has completely vanished. At the same time, nascent and disappearing spiral states near critical lines also catalyze topological charge changing processes and thus may lead to the formation and destruction of skyrmionic states at low temperatures. In this respect the tilted spiral phase may introduce domain walls and other inhomogeneous textures that would act as seeds for the nucleation of skyrmions.

In the present paper, we address a problem of skyrmion nucleation in a bulk cubic helimagnet Cu_2OSeO_3 by focusing on the internal structure of domain walls (DW) between differently oriented helical domains. In the next section (Sec. II), we discuss the experimental phase diagrams obtained for decreasing and increasing magnetic fields, which exhibit the LT skyrmion stability regions with respect to the critical lines of the spiral transformations. These highlight two plausible scenarios for skyrmion nucleation—(i) via ruptures of metastable spiral domains with their wave vectors perpendicular to the field and (ii) from the domain boundaries between tilted spiral states.

In Sec. III, we introduce our phenomenological model and the algorithms used for our simulations (Sec. III A). We then discuss the internal structure of the conical and helical states, as deduced within the isotropic theory, as well as their stability lines or characteristic fields. These states are essentially modified by the cubic anisotropy (Sec. III B), and this phenomenon underlies the skyrmion stability at the deduced theoretical phase diagram (Sec. III C).

In Sec. IV, we examine theoretically the internal structure of domain walls between spiral domains with mutually perpendicular wave vectors. We discuss a wide variety of such DWs by systematically considering all possible combinations of the wave vectors in the neighboring helical domains as well as their vertical and/or horizontal orientation. We show that skyrmionic nuclei of different types may arise within these DWs and thus endow them with a finite topological charge, permitting a potential coupling to spin currents and contributions to the topological Hall effect. Skyrmion varieties within the DWs include not only conventional skyrmion tubes oriented along the field (which form the most stable SkLs), but also two types of horizontal skyrmions perpendicular to the field, which may additionally couple/zip helical domains due to their mutual attraction [34].

Subsequently in Sec. V, we examine domain walls between tilted spiral states. The results of numerical simulations are

applied to analyze recent experimental findings in different chiral magnets and liquid crystals (Sec. VI). The paper finally discusses the most likely mechanism that would account for the experimental findings obtained for the bulk helimagnet Cu_2OSeO_3.

II. EXPERIMENTAL PHASE DIAGRAMS AND THE QUESTION OF SKYRMION NUCLEATION

In the present section, we discuss experimental results obtained on the bulk cubic helimagnet Cu_2OSeO_3, which are the starting point of this work. The sample was the same as the one used in our previous work [14,15], although we made experiments anew to eliminate some small shortcomings of the previous measurements. Figures 1(a) and 1(b) show the phase diagrams derived from small angle neutron scattering (SANS) for $\mathbf{H}||[001]$ measurements after used zero-field cooling (ZFC) the sample from $T > T_C$ to the temperature of interest. In this configuration the ground state at zero field consists of spiral domains with mutually perpendicular propagation directions [Fig. 1(c)] along the easy directions of the cubic anisotropy $\langle 100\rangle$, in agreement with experiment. Then, DWs should be formed at the boundaries between spiral domains. For $\mu_0\mathbf{H}||[001]$ only one domain should represent the most energetically favorable state but the other metastable spirals would flip along the field only at the critical field H_{C1}. Hence, the DW-related topology should be preserved for $H < H_{C1}$. Furthermore, for $H > H_{C1}$ and $T \lesssim 30\,K$, the helices tilt toward the $\langle 111\rangle$ crystallographic directions, thus away from the magnetic field direction leading to the tilted spiral (TS) phase. The TS phase is multidomain, with DWs formed between the energetically equivalent domains. TS represents a remarkable deviation from the generic phase diagram of cubic chiral magnets. At low temperatures, $T \lesssim 15\,K$, this phase extends over the whole region that is usually ascribed to the conical phase, i.e., for $H_{C2} > H > H_{C1}$. In this temperature range, where also the intensive LT skyrmionic scattering appears, H_{C1} marks the transition between two different multidomain phases, the helical and TS phase, and not between a multidomain helical and a single domain conical phase, as it is the case for other cubic chiral magnets, and also for Cu_2OSeO_3 when the magnetic field is applied along the other main crystallographic directions.

Magnetic fields also stabilise skyrmions leading to the characteristic scattering the extend and intensity of which is summarized by the blue areas in Figs. 1(a) and 1(b): deep dark blue for the HT A-phase, dark blue for the intense LT skyrmionic scattering, and light blue for the weak scattering that surrounds both the LT and HT skyrmion pockets and connects them. Skyrmionic scattering thus appears over large areas of the phase diagram and shows a clear hysteretic behavior, that sets in already below 55 K, i.e., just below the pocket of the A-phase. Indeed this scattering concentrates around the H_{C2} line when the magnetic field increases from zero to above H_{C2}, and around the H_{C1} line when the magnetic field subsequently decreases from above H_{C2} to zero.

Based on these experimental findings in Cu_2OSeO_3 we infer that skyrmion nucleation may occur via the following mechanisms [14]:

(i) Thermodynamically stable skyrmions may form from domain boundaries between *stable* (with wave vectors parallel to the field) and *metastable* spiral states with wave vectors perpendicular to the field. Such a nucleation process may occur for both increasing and decreasing magnetic fields [see a schematic in Fig. 1(c)]. In the first case, one immediately gets three spiral domains oriented along $\langle 100\rangle$ after zero-field cooling procedure. In the second case, one recovers the spiral domains due to the small misalignment of the sample with respect to the field.

(ii) Skyrmions may nucleate at the domain boundaries between domains of the tilted spiral states slanting toward the easy $\langle 111\rangle$-axes of the anisotropic exchange [see schematic in Fig. 1(d)]. Such a nucleation process may also occur with increasing or decreasing magnetic field.

In both cases triangular arrays of skyrmions are energetically favorable as compared with both the tilted and conical spiral states. These experimental findings and considerations motivate the study of the structure of domain boundaries between helical/spiral domains, which may nucleate thermodynamically stable skyrmions or even skyrmion lattices.

III. PHENOMENOLOGICAL THEORY OF SKYRMION STABILITY IN BULK CUBIC HELIMAGNETS

A. Isotropic micromagnetic energy functional

Our numerical simulations (temperature annealing and a single-step Monte Carlo dynamics using the METROPOLIS algorithm) are based on the Dzyaloshinskii model for magnetic states in cubic noncentrosymmetric ferromagnets [18,19] and include only the main interactions necessary to stabilize modulated states:

$$W(\mathbf{m}) = (\mathbf{grad}\,\mathbf{m})^2 + w_D - \mu_0 M\mathbf{m}\cdot\mathbf{h}. \qquad (2)$$

Here, we use reduced values of the spatial variable, $\mathbf{x} = \mathbf{r}/L_D$, where $L_D = A/D$ is the periodicity of the modulated states. A and D are the exchange stiffness and the Dzyaloshinskii constant, respectively, and the sign of D determines the sense of the magnetization rotation. $\mathbf{m} = (\sin\theta\cos\psi;\sin\theta\sin\psi;\cos\theta)$ is the unity vector along the magnetization vector $\mathbf{M} = \mathbf{m}M$, and $\mathbf{h} = \mathbf{H}/H_D$ with $\mu_0 H_D = D^2/(AM)$ is the reduced value of the applied magnetic field. The cubic and exchange anisotropy constants are given by $k_c = K_c A/D^2$ and $b_{\rm ea} = B_{\rm ea}/A$, respectively.

The numerical methods on the energy minimization procedure which leads to solutions for different modulated states are explicitly described in, e.g., Ref. [20] and hence will be omitted here. We just mention that the Euler-Lagrange equations derived from the energy functional (2) are nonlinear partial differential equations. These equations can be solved by numerical energy minimization procedure using finite-difference discretization on rectangular grids with adjustable grid spacings and periodic boundary conditions. The components (m_x, m_y, m_z) of the magnetization vector $\mathbf{m}$ have been evaluated in the knots of the grid, and for the calculation of the energy density (2) we used finite-difference approximation of derivatives with different precision up to eight points as neighbours. To check the stability of the numerical routines we refined and coarsened the grids and varied the grid spacings Δ_y and Δ_x.

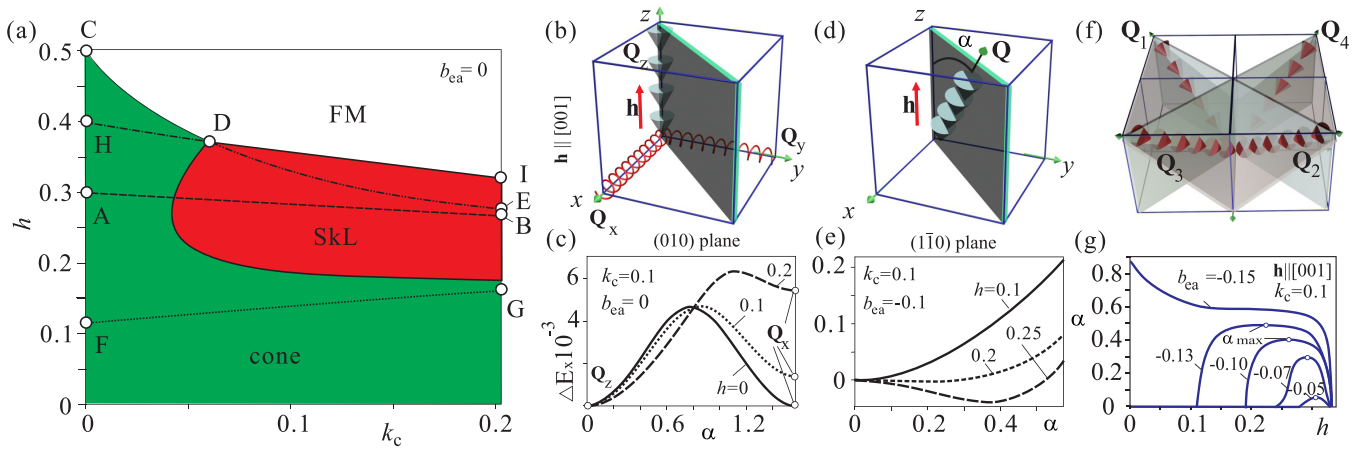

FIG. 2. (a) Phase diagram of the ground states derived from the model (2) for an applied magnetic field **h**||[001] and zero anisotropic exchange (1). The regions of the thermodynamical stability are colored red (skyrmions), green (cones), and white (saturated state). A-B and H-I are the lability lines of the spiral and skyrmion phases. C-D-E is the line of the first-order phase transition between the conical and the homogeneous states. At the dotted line F-G the energy of SkL becomes equal to the energy of the metastable helical spiral states with the wave vectors along the [100] and [010] directions. (b–g) Spiral reorientation for **H**||[001]. (b) Schematics of three spiral domains in low magnetic fields. At zero field, the spiral energy is degenerate with respect to the propagation vector. (c) Dependence of the spiral energy density on the wave vector **Q** varying in the (010) plane at zero field and at $h = 0.1$; 0.2. The global energy minimum is reached at $\mathbf{Q}_z$[001] immediately as the field is applied (α is given in radians). The local minimum corresponding to metastable spirals with their propagation perpendicular to the field persists up to relatively high field values. (d) Schematics of a tilted-spiral state that appears above a critical value of the magnetic field, in which **Q** rotates away from the magnetic field vector toward the ⟨111⟩ directions. (e) Energy density plotted as a function of the tilt angle α in the (110) plane for several field values. (f) Schematics showing enumeration of wave vectors in the domains of a tilted spiral state. (g) Magnetic field dependence of the angle α describing the tilt of the spiral wave vector **Q** away from **h**||[001] toward the body diagonals for different values of $|b_{ea}|$. Above some critical value, α increases from 0, which corresponds to the conical spiral phase, to a maximal value, α_{max}, and then decreases back to 0 as the magnetic field strength, h, increases. For $b_{ea} > 0.14$, **Q**||⟨111⟩ even at zero field and smoothly rotates toward [001] with increasing field.

In the general case of cubic helimagnets, the Dzyaloshinskii-Moriya interaction (DMI) assumes the following form [1,18]:

$$w_D = \mathcal{L}^{(x)}_{y,z} + \mathcal{L}^{(y)}_{x,z} + \mathcal{L}^{(z)}_{x,y} = \mathbf{m} \cdot \mathrm{rot}\mathbf{m}, \tag{3}$$

and it includes the Lifshitz invariants (LI), $\mathcal{L}^{(k)}_{i,j} = m_i \partial m_j/\partial x_k - m_j \partial m_i/\partial x_k$. These energy terms involve first derivatives of the magnetization with respect to the spatial coordinates x_i along all coordinate axes.

B. One-dimensional spiral modulations within the isotropic theory

In chiral magnets the Dzyaloshinskii-Moriya interactions w_D play a crucial role in destabilizing the homogeneous ferromagnetic arrangement and twisting it into a helix. At zero magnetic field the helices are single-harmonic modes forming the global minimum of the functional $W(\mathbf{m})$ [18], $\mathbf{M} = M_s[\mathbf{n}_1 \cos(\mathbf{q}\cdot\mathbf{r}) + \mathbf{n}_2 \sin(\mathbf{q}\cdot\mathbf{r})]$. $\mathbf{n}_1$, $\mathbf{n}_2$ are the unit vectors in the plane of the magnetization rotation orthogonal to the wave vector $\mathbf{q} = \mathbf{n}_3/L_D$ with $\mathbf{n}_3 \perp \mathbf{n}_2 \perp \mathbf{n}_1$ (i.e., $\mathbf{n}_1$, $\mathbf{n}_2$, and $\mathbf{n}_3$ are three mutually orthogonal unit vectors). The helical modulations have a fixed rotation sense determined by the sign of Dzyaloshinskii-Moriya constant D and are continuously degenerate with respect to the propagation directions of the helical modulations in space. An applied magnetic field lifts this degeneracy and stabilizes two types of one-dimensional modulations: cones and helicoids with propagation directions parallel and perpendicular to the applied magnetic field, respectively.

For helicoids, analytical solutions for the polar angle $\theta(x)$ of the magnetization written in spherical coordinates, $\mathbf{M} = M_s[\sin\theta(x)\cos\psi, \sin\theta(x)\sin\psi, \cos\theta(x)]$, are derived by solving a *pendulum* equation $Ad^2\theta/dx^2 - H\cos\theta = 0$. Such solutions are expressed as a set of elliptical functions [18] and describe a gradual expansion of the helicoid period with increased magnetic field (see the set of angular profiles $\theta(x)$, e.g., in Fig. 4.1. of Ref. [21]). In a sufficiently high magnetic field H_H the helicoid infinitely expands and transforms into a system of isolated noninteracting 2π-domain walls (kinks) separating domains with the magnetization along the applied field [2,18]. The dimensionless value of this critical field is $h_H = H_H/H_D = \pi^2/8 = 0.30843$ [point A at the phase diagram, Fig. 2(a)]. The azimuthal angle ψ, on the contrary, is fixed by the different forms of the Lifshitz invariants. In particular $\psi = \pi/2$ for Bloch helicoids in cubic helimagnets and $\psi = 0$ for Neel helicoids or cycloids in polar skyrmion hosts with C_{nv} symmetry such as the lacunar spinels GaV_4S_8 [22], GaV_4Se_8 [23], or $VOSe_2O_5$ [24].

The conical state combines the properties of the ferromagnetic and the helical states and results from the competition between the Zeeman and DMI energies. The conical spirals retain their single-harmonic character with $\psi = z/2L_D$ and $\cos\theta = 2|\mathbf{H}|/H_D$. The magnetization component along the applied field has a fixed value $M_\perp = M\cos\theta = 2MH/H_D$ and the magnetization vector **M** rotates within the surface of a cone. The critical value $h_d = 2H_D$ marks the saturation field

of the conical state [point C at the phase diagram, Fig. 2(a)]. For the functional $W(\mathbf{m})$ in Eq. (2), the conical phase is the global minimum over the whole range of magnetic fields where modulated states exist ($0 < h < h_d$), whereas helicoids and skyrmion lattices can exist only as metastable states.

C. Phase diagram in the presence of magnetocrystalline cubic anisotropy

To ensure skyrmion stability for *bulk* cubic helimagnets, we supply the model (2) with small anisotropic contributions (1) [12], which lead to a deformation of the conical phase. References [12,21] provide comprehensive overviews of the structure of all modulated structures in the presence of the cubic and exchange anisotropies, their field-driven transformation, and the corresponding theoretical phase diagrams. In particular, the stabilization effect of cubic anisotropy on SkL becomes apparent for the cases of the first-order phase transition at H_{C2} between the cones and the homogeneous state [line C-D-E in the phase diagram, Fig. 2(a)].

Figure 2(a) shows the zero-temperature phase diagram in the (k_c, h) plane calculated for $b_{ea} = 0$, which contains the conical state with the propagation vector $\mathbf{q}||\mathbf{H}||[001]$ (green color), the skyrmion lattice phase (red color) and the field-polarized phase (white color). Cones, i.e., modulated states with a negative energy relative to the homogeneous state, exist below the line C-D-E. At this line the cones flip into the saturated state by a first-order phase transition as described in Ref. [12]. Cones are only thermodynamically stable within the region filled with a green color whereas they are metastable in the remaining part of their stability region. Helicoids may exist below the line A-B (the field H_H), above which they turn into the homogeneous state. For the considered anisotropy values, helicoids do not gain thermodynamical stability (although for higher anisotropy values, a pocket with the stable spiral states appears at the phase diagram; see Ref. [12] for details). However, skyrmions gain stability already for relatively small values of $k_c \approx 0.04$ and are metastable in a much wider region of the phase diagram. The dotted line F-G in Fig. 2(a) marks the magnetic field at which the energy of skyrmions for a given k_c becomes equal to the energy of the metastable helical spiral states with the wave vectors along the [100] and [010] directions. Skyrmions transform into the homogeneous state along the H-I line. This transition occurs before the cone suppression at the line H-D, and after it, along the D-I line. In fact, due to the strong influence of the cubic anisotropy on the conical phase, for the critical anisotropy value $k_c(D)$ skyrmions can persist up to higher fields than the cones.

We also notice the point D at the experimental phase diagram [Fig. 1(a)]—an intersection point between the curve H_{C2} and an upper boundary of a LT-SkL pocket—that demarcates two temperature regimes: for lower temperatures, SkL exists above H_{C2} and its nucleation is believed to be directly related to the stability region of an oblique spiral [13,14]; for higher temperatures, SkL dissolves before the cone saturation field H_{C2}; at the same time, identification of an oblique spiral in this temperature interval bumps into the accuracy of experimental procedures. According to the theoretical phase diagram [Fig. 2(a)], the point D corresponds to the value $k_c^{(D)} \approx 0.06$. Nonetheless, it cannot be used as a reference point to contrast both phase diagrams. In experiments, the stability region of LT skyrmions strongly depends on the prehistory and nucleation mechanisms and thus is different for the decreasing [Fig. 1(b)] or increasing [Fig. 1(a)] magnetic fields. Moreover in the experiments, skyrmions "feel" the impact of exchange anisotropy omitted in the theoretical phase diagram. Still, point D introduces an important threshold related to the behavior of an oblique spiral discussed in the previous section. The contribution of an exchange anisotropy to the cone energetics is rather negligible for $\mathbf{h}||[001]$ and is related to the small variation of the m_z component along z [12]. Thus, based on the increasing value of H_{C2} with increasing temperature (see Fig. 1) one may conclude that the cubic anisotropy k_c weakens. In the following numerical simulations, we will use $k_c = 0.1$ and $h = 0.25$, which correspond to a low-temperature region of the experimental phase diagram [Fig. 1(a)] to the left from point D.

IV. SKYRMION NUCLEATION FROM METASTABLE SPIRAL DOMAINS

For $\mathbf{H}||[001]$, only the spirals with $\mathbf{Q}_z||[001]$, represented by the blue cones in Fig. 2(b), are stable whereas the spirals with $\mathbf{Q}_x||[100]$ and $\mathbf{Q}_y||[010]$, represented by red springs, become metastable. Figure 2(c) depicts the dependence of the spiral energy on the angle α, between $\mathbf{Q}$ and the [001] axis, for $\mathbf{Q}$ varying in the (010) plane. In this figure, the $\mathbf{Q}$ vectors of all three spirals are marked separately to distinguish their energies. At low fields, the wave vectors of the metastable spirals remain parallel to [100] and [010]. However, these states become eventually unstable at rather high magnetic fields, when the respective energy minima disappear. In real experiments, however, these spirals should be able to overcome the energy barrier and thus "jump" along the direction of the magnetic field, a transition that should further be facilitated by the energetic cost of domain walls to the conical state.

The line F-G at the theoretical phase diagram corresponds to the phase transition between the extended SkL and the spiral state along [100]. Thus, metastable spiral domains may, via rupture, give rise to thermodynamically stable skyrmions [14,25], which subsequently form clusters within the conical state. This mechanism also observed in the first papers on skyrmion visualization [26,27] also leads to pairs of merons that behave as if they were free particles, independent of each other. The properties of such skyrmions and merons, embedded in the spiral background, were recently investigated in Ref. [28]. The essential difference is that in the present case spiral states are metastable solutions, which nonetheless can give rise to a thermodynamically stable skyrmions.

A. Vertical domain boundaries between cones $\mathbf{Q}_z$ and helicoids $\mathbf{Q}_y$

Figure 3 shows a domain boundary between spiral domains $\mathbf{Q}_z$ and $\mathbf{Q}_y$ [see also schematics in Fig. 3(e)]. The Figure shows different cross-sections in the planes xy and xz as color plots of the corresponding magnetization component (see the color scales adjacent to all panels) with the arrows being the projections onto the considered planes. These plots show that the domain boundary is located in the plane yz with

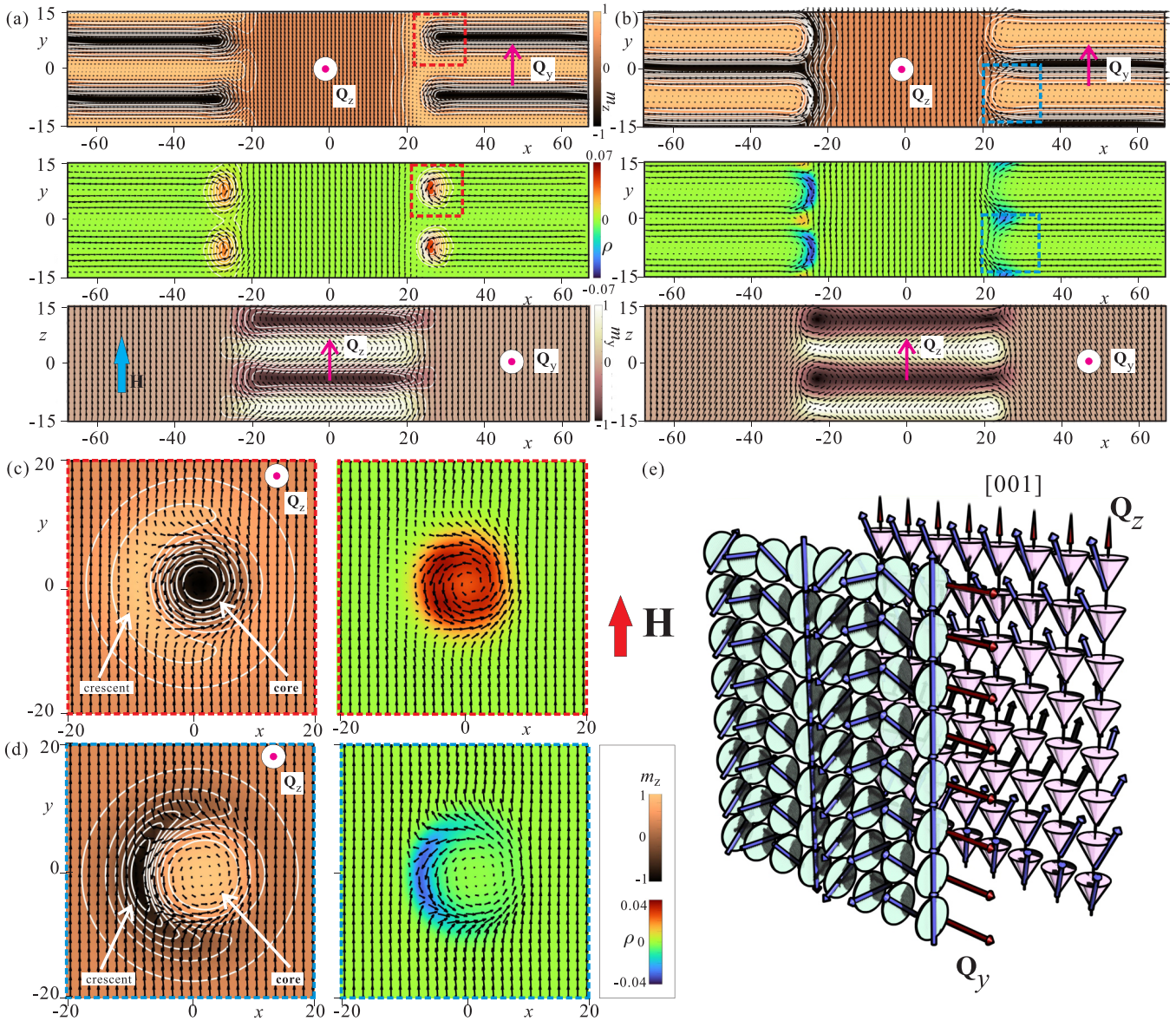

FIG. 3. Phase boundary between domains of a conical $\mathbf{Q}_z$ and a helical phase $\mathbf{Q}_y$. $h = 0.25$, $k_c = 0.1$, and $b_{\rm ea} = 0$. Different cross-sections are shown as two-dimensional color plots of the corresponding magnetization component with the arrows being the projections of the magnetization on to the plane. The domain boundaries may give rise to half-skyrmions with negative (a) and positive (b) polarity of their cores. Consequently, the topological charge density [second row in panels (a) and (b)] exhibits either a positive or a negative pattern. The corresponding half-skyrmions can be considered as "fragments" of isolated skyrmions with the unitary topological charge surrounded by the conical phase (c, d). Both skyrmion varieties are characterized by the split structure consisting of the circular core and a bent crescent. Only the skyrmions in panel (c) may form a stable skyrmion lattice, whereas those in panel (d) eventually collapse. (e) Schematics showing coexisting domains of the stable conical phase $\mathbf{Q}_z$ and a metastable helicoid with the wave vector $\mathbf{Q}_y$.

some finite width along x. We notice that the present DW is truly three-dimensional and varies along the z axis.

The DW hosts a meronlike structure with the meron axes along z, and the merons hold either positive [Fig. 3(a)] or negative [Fig. 3(b)] topological charges depending on the magnetization orientation in the meron centers. The topological charge density ρ thus characterizes the topology of a magnetization distribution and within the xy plane is defined as

$$\rho = \frac{1}{4\pi}\mathbf{m}\left(\frac{\partial \mathbf{m}}{\partial x} \times \frac{\partial \mathbf{m}}{\partial y}\right). \tag{4}$$

This definition can easily be generalized for other cross-sections, which will be considered in the following.

We encompass the corresponding merons by squares with the dashed lines colored according to their topological charge: red for positive and blue for negative. The frontal parts of these merons in the wall have a similar structure as those of so-called nonaxisymmetric skyrmions [31,32] [Figs. 3(c) and 3(d)] and play the role of nuclei for skyrmion clusters with an hexagonal arrangement. The conical phase $\mathbf{Q}_z$ underlies the attractive interaction between such skyrmions [28] and this explains the formation of skyrmion clusters observed in the experiments on thin-films [28] and bulk systems of

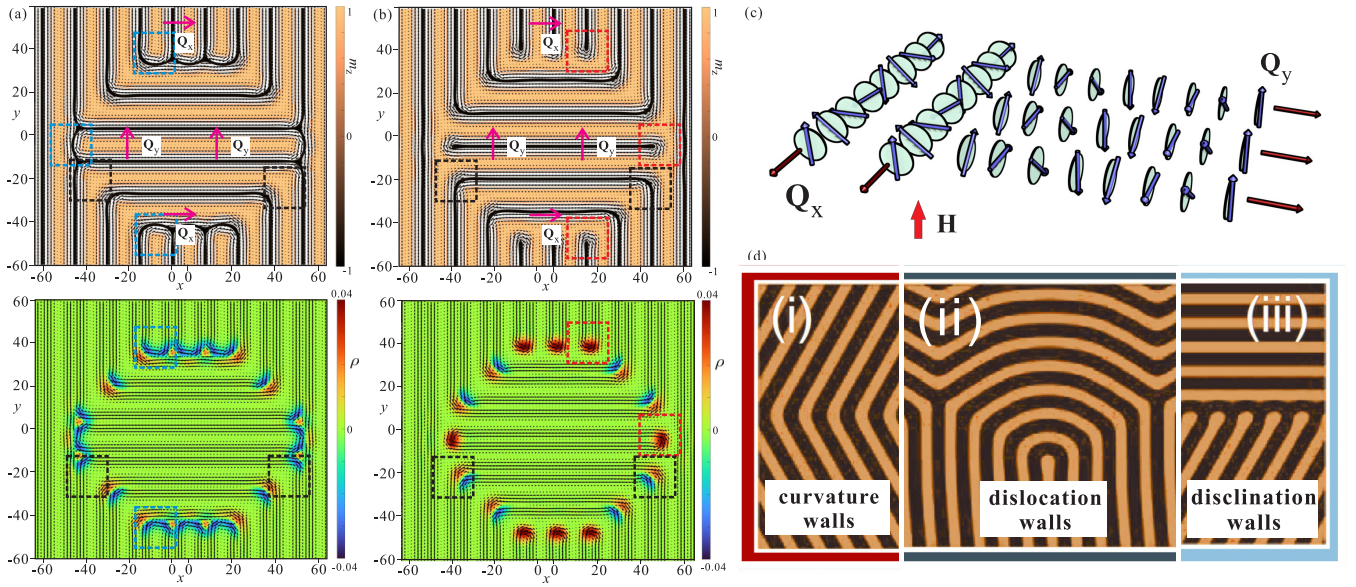

FIG. 4. Phase boundary between metastable spiral domains with the in-plane orientation of their wave vectors shown as distributions of the magnetization (first row) and of the topological charge (second row) for opposite polarities of half-skyrmions (a, b). $h = 0.25$, $k_c = 0.1$, $b_{ea} = 0$. (c) Schematics showing coexisting spiral domains with the wave vectors $\mathbf{Q}_x$ and $\mathbf{Q}_y$. The general domain boundaries depicted in panels (a, b) include parts of curvature, disclination, and dislocation walls (c) introduced in Ref. [33].

Cu_2OSeO_3 [14]. The conical phase stabilized by the Lifshitz invariants along z axis in chiral magnets presumably does not have any counterpart in the systems with other stabilization mechanisms such as dipole-dipole interactions [29] and/or the interplay of elastic, electrostatic, and gradient energies [30]. Thus, it would be a rather questionable endeavor to realize 3D domain walls in the mentioned systems. The experimental observation of such domain walls also poses an experimental challenge since it would require resolving the 3D structure in bulk helimagnets.

The internal spin patterns of isolated skyrmions with their axes along the wave vector of the conical phase are depicted in Figs. 3(c) and 3(d). In general, the magnetization distribution along a cross-section xy splits into the central core region that nearly preserves the axial symmetry and the transient region, connecting the core with the embedding conical state. This part of the skyrmion cross-section is *asymmetric* and acquires a crescent-like shape, which undergoes additional screwlike modulation along z axis, matching the rotating magnetization of the conical phase. Depending on the orientation of the magnetization in the centers of skyrmion cores [i.e., opposite (c) or along the field (d)], one may distinguish two skyrmion varieties with opposite topological charges. In particular, the topological charge density is concentrated within the skyrmion core for the so-called minus-skyrmions [Fig. 3(c)], whereas it is located at the crescent part for the plus-skyrmions [Fig. 3(d)]. Additional details on the internal structure of such skyrmions and the mechanism leading to their attraction can be found in Refs. [20,28].

B. Domain boundaries between in-plane helicoids $\mathbf{Q}_x$ and $\mathbf{Q}_y$

The same skyrmion types (encompassed by blue and red squares) may appear within domain walls between the $\mathbf{Q}_x$ and $\mathbf{Q}_y$ spiral domains [see also schematics in Fig. 4(c)] with the wave vectors oriented in the xy plane (Fig. 4).

The more general DWs, however, may avoid any skyrmion formation, since the wave vector may just smoothly bend from one domain to another. Spatial variations of the helix axis $\mathbf{Q}$ are dictated by the easy $\langle 100 \rangle$ axes of the cubic anisotropy and result in a curvature of the helical spin structure. When the space is filled with helices, the wave vectors of which rotate by 90° at the domain boundaries, vortices that break the periodicity arise spontaneously. The resulting spin distributions shown in Fig. 4 were obtained under constriction of the periodic boundary conditions: the $\mathbf{Q}_y$ spiral domain is surrounded by a $\mathbf{Q}_x$ domain.

The circular curved parts within the domain walls contain coupled positive and negative topological charges as shown by the encompassing black squares with dashed boundaries. The corresponding DWs were dubbed "curvature walls" in Ref. [33] [Fig. 4(d)]. Figure 4(a) also incorporates "zigzag" disclination walls and "dislocation" walls [33]. For convenience, we sketch the corresponding DW-types from Ref. [33] in Fig. 4(d). The strength of the vortices is parametrized by the winding angle of the helix axis on a path encircling the vortex core and results in their half-integer topological charge. In the isotropic case, it was shown that the energy of the mentioned DWs drastically depends on the angle between the wave vectors of helical domains [33]. Here we refrain from the corresponding simulations, that would include cubic and exchange anisotropies, and tacitly consider that the wave vectors point to the easy cubic directions as experimentally observed, e.g., for the bulk helimagnet Cu_2OSeO_3. Finally, it is important to note that such domain boundaries with a finite topological charge are in general expected to give rise to emergent electrodynamics for both electrons and magnons and thus contribute to a topological Hall effect.

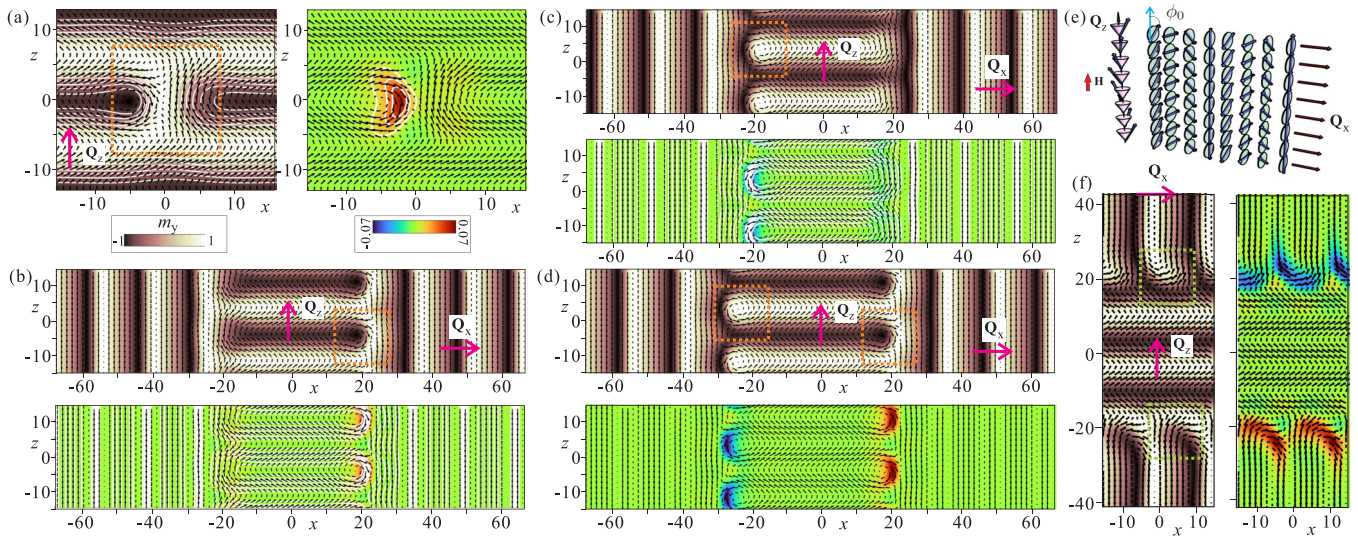

FIG. 5. Phase boundary between the spiral domains $\mathbf{Q}_z$ and $\mathbf{Q}_x$ leading to horizontal half-skyrmions of two varieties as defined by the boundary orientation in the vertical plane yz (b–d) or the horizontal plane xy (f). $h = 0.25$, $k_c = 0.1$, and $b_{\rm ea} = 0$. (e) Schematics showing coexisting spiral domains with the wave vectors $\mathbf{Q}_x$ and $\mathbf{Q}_z$. The horizontal skyrmion of the first type (a) represents a cut of a conical state with $\mathbf{Q}||\mathbf{H}$, whereas the horizontal skyrmion of the second type (f) is a cut of the helical state with $\mathbf{Q}\perp\mathbf{H}$. Depending on the phase ϕ (e) of the rotating magnetization in neighboring spiral domains, the topological charge density exhibits different distribution patterns either with the total positive (b), negative (c), or zero (d) topological charge as computed in the xz plane.

We also note that the same 2D DWs are realized for different stabilization mechanisms of skyrmions beyond DMI, such as the interplay of elastic, electrostatic and gradient energies [30], and/or dipole-dipole interactions [29]. However, these correspond to different branches of solutions, which possess different properties and should be treated cautiously. Furthermore, as stated before, in those systems it would be difficult to realize a conical spiral phase, which is at the core of the effects discussed in the present manuscript.

C. Domain boundaries between cones $\mathbf{Q}_z$ and helicoids $\mathbf{Q}_x$

Domain boundaries between helical domains may give rise also to skyrmion tubes oriented perpendicular to the field (Fig. 5). This is indeed the case for the spiral domains $\mathbf{Q}_z$ and $\mathbf{Q}_x$ [see schematics in Fig. 5(e)]. Vertical DWs between these spiral domains can nucleate horizontal skyrmions of the first type [Fig. 5(a)]. These skyrmions arise from a rupture of a spiral with its $\mathbf{Q}$ vector along the field and have a nonaxisymmetric structure [encompassed by an orange-colored rectangle in Fig. 5(a)]. They run along the y axis and develop a topological charge in the plane xz [right panel of Fig. 5(a)]. At zero magnetic field, these skyrmions perfectly blend into the spiral state and represent a pair of merons with equally distributed topological charge $Q = 1/2$. At higher fields, they adopt nonaxisymmetric structures in the xz plane and their topological charge accumulates at their core similar to the skyrmions shown in Fig. 3(c). These horizontal skyrmions may exist with positive and negative polarities, i.e., directions of the magnetization in the region between two cylinders. For additional details on the properties of the horizontal skyrmions refer to Refs. [20,34].

The creation of such skyrmions within the domain boundaries is specified by the phase shift of helical domains ϕ_0 [Fig. 5(e)]. In the most symmetric cases, the topological charge is either positive [Fig. 5(b)] or negative [Fig. 5(c)] and shifts to one side. An alternating pattern can also be realized [Fig. 5(d)]. A similar behavior can also occur for the vertical skyrmions shown in Fig. 3 [see third row in panels (a) and (b)]. Such magnetization distributions also minimize the energy density with respect to ϕ_0.

Horizontal DWs between spiral domains $\mathbf{Q}_z$ and $\mathbf{Q}_x$ may nucleate horizontal skyrmions of the second type [encompassed by the green-colored rectangle in Fig. 5(e)]. These skyrmions are simply a rupture of a spiral state with its $\mathbf{Q}$-vector perpendicular to the field. They were first introduced in Ref. [20], where it was shown that their energy becomes negative with respect to the spiral state near the critical field H_H [line A-B at the phase diagram, Fig. 2(a)] when the corresponding spiral disappears. Moreover, it was concluded that besides the obvious squarelike or hexagonal-like arrangement of merons, one may consider the emergence of more entangled spin structures. As a basis for these configurations, one may also consider crosslike states obtained by the intersection of two horizontal skyrmions with opposite polarities and having positive or negative diagonals as their main elements (see Fig. 6 in Ref. [20]).

With decreasing magnetic field only the conical domain with $\mathbf{Q}_z||[001]$ survives, i.e., the other spiral domains along [100] and [010] are not recovered. Thus, such a nucleation mechanism via metastable spiral domains becomes unlikely under these conditions.

V. SKYRMION NUCLEATION FROM DOMAINS OF AN OBLIQUE SPIRAL STATE

The interplay between competing anisotropic spin interactions (1) may also give rise to tilted spiral states with rather

smooth variation of the tilt angle [Figs. 2(d)– 2(g)]. For the present setup of easy anisotropy axes (i.e., easy axes ⟨100⟩ for the cubic anisotropy and easy axes ⟨111⟩ for the anisotropic exchange), the tilted spiral state is found only for $\mathbf{H} \parallel [001]$. Above a critical field value, the conical spiral $\mathbf{Q}_z$ begins to tilt toward one of the four body diagonals, the ⟨111⟩ directions, as shown in Fig. 2(d). Such a tilted spiral state appears when $|b_{\rm ea}|$ exceeds a critical value. As an illustration, we performed simulations for a fixed value of the cubic anisotropy $k_c = 0.1$ while varying $b_{\rm ea}$. In this case the critical value was found to be slightly lower than $b_{\rm ea} = 0.05$.

Figure 2(e) shows the dependence of the spiral energy on the tilt angle α with $\mathbf{Q}$ varying in the $(1\bar{1}0)$ plane, for $h = 0.1,\ 0.2,$ and 0.25. Although for $h = 0.1$ the wave vector still points along the field ($\alpha = 0$), for $h = 0.2$ it starts to deflect, and the energy dependence acquires a "shallow" minimum. For $h = 0.25$, the minimum becomes more pronounced and is energetically well distinguishable from the conical state. As h increases, the angle α grows, reaches its maximal value and then decreases back to zero, corresponding to a return into the conical spiral state [Fig. 2(g)]. The maximal tilt angle, $\alpha_{\rm max}$ depends on the ratio of the competing fourth-order and exchange anisotropies. As the exchange anisotropy increases above the critical value, $|b_{\rm ea}| > 0.14$, the state with $\mathbf{Q} \parallel \langle 111 \rangle$ is stabilized even at zero magnetic field. We notice, however, that such a behavior of a tilted spiral is inherent only for the chosen value of the cubic anisotropy. For larger values of k_c, the spiral state undergoes a first-order phase transition with respect to the homogeneous state (to be published).

Figure 6 shows the structure of domain walls between oblique spirals with their wave vectors within the (110) plane. Similar to the case of spiral domains in Fig. 4, such DWs may in general contain horizontal half-skyrmions running along [110] directions (called vortices in Refs. [33,35]) as well as curved vortex-free parts continuously merging two spiral domains. Just as was pointed out for DWs in Figs. 5(b)–5(d), the pattern of the topological charge density within the $\mathbf{Q}_2$ domains is specified by the relative phases of spiral states. One may also distinguish two varieties of horizontal skyrmions.

To nucleate a stable SkL with the skyrmion axes along the field, however, one should consider DWs between oblique spiral domains $\mathbf{Q}_2$ and $\mathbf{Q}_3$ [Fig. 2(f)], which lie in the plane [011] (will be addressed elsewhere). In an ideal case, one may envision oblique skyrmion tubes, which tilt toward the field with the increasing angle α of oblique spirals, i.e., the larger spiral deflection from the field facilitates creation of "correct" skyrmions for building stable SkL. Alternatively, one might model spiral superstructures formed by rotating wave vectors from one domain of an oblique spiral to another. Such an inhomogeneous magnetization environment may plausibly give rise even to fully three-dimensional particle-like states like hopfions or torons containing point defects.

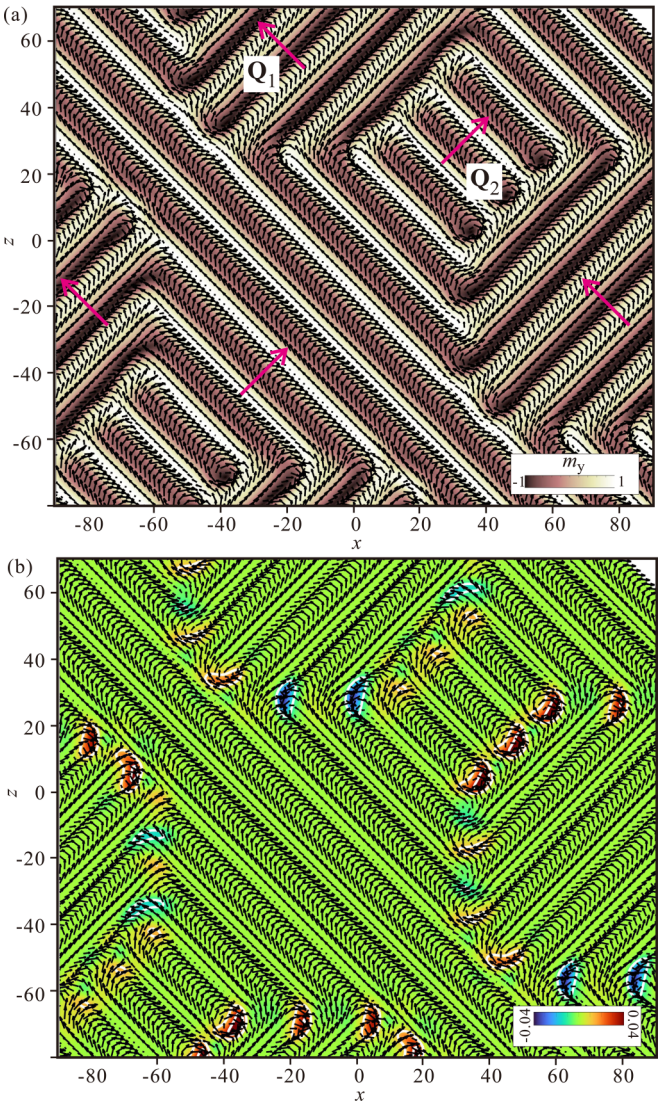

FIG. 6. Phase boundary between domains of an oblique spiral state with the wave vectors $\mathbf{Q}_1$ and $\mathbf{Q}_3$ within the $(1\bar{1}0)$ plane, which may result in horizontal skyrmions running along y axis. $h = 0.25$, $k_c = 0.1$, and $b_{\rm ea} = -0.1$. Oblique skyrmions, on the contrary, may arise within the boundaries between, e.g., $\mathbf{Q}_1$ and $\mathbf{Q}_2$ (will be computed elsewhere).

VI. DISCUSSION: EXPERIMENTAL EVIDENCE OF A DOMAIN-WALL CONFINED TOPOLOGY

In the following we discuss recent experiments on chiral magnets that provide evidence for the existence of domain walls between spiral domains, similar to those modeled numerically in the previous sections. We start from direct (mainly through imaging) observations in chiral magnets and liquid crystals and proceed to results obtained indirectly (through bulk measurements or scattering) on bulk cubic helimagnets.

A. Attracting skyrmions within the conical phase in B20 helimagnets

The attractive interaction between magnetic skyrmions mediated by the conical phase and their cluster formation has been observed experimentally in thin (70 nm)

single-crystal samples of Cu_2OSeO_3 using transmission electron microscopy [28]. The reported skyrmion configuration corresponds to the domain boundary considered in Fig. 3. Other cluster configurations have also been detected including even a squarelike arrangement of skyrmions (as shown by a snapshot of Fig. 2(a) in Ref. [28]). The visualization of such DWs is of course an experimental "tour de force," which however could not resolve the subtleties of the DW structure. Furthermore, in this experiment the structure of isolated skyrmions and their clusters were modified by so called surface twists where the magnetization changes its helicity toward the surface [36,37]. Such surface twists may lead to an anisotropic skyrmion attraction and to the formation of skyrmion chains. And indeed, all videos of Ref. [28] show skyrmions in constant motion. This may be caused either by the electron beam or by frustration, as skyrmions attempt to minimize the anisotropic interskyrmion attraction.

Direct evidence of the field-dependent character of the interaction between individual magnetic skyrmions as well as between skyrmions and edges in B20-type FeGe nanostripes was also reported in Ref. [38]. Skyrmion clusters were observed by means of high-resolution Lorentz transmission electron microscopy. It was shown that above a critical values of an external magnetic field the character of long-range skyrmion interactions changed from attraction to repulsion, in quantitative agreement with micromagnetic simulations [39].

Domain walls between helical domains with in-plane orientation of their wave vectors (Fig. 4) have been recently observed in the near-room-temperature chiral magnet iron germanium (FeGe; $T_C = 278$ K) using magnetic force microscopy [33]. These helimagnetic domain walls have a complex but well-defined inner structure, consistent with the one shown in Fig. 4. Such vortex domain walls were also considered theoretically in early publications in skyrmionics [35] to explain the experimental results obtained in thin-layered systems of $Fe_{0.5}Co_{0.5}Si$ [40]. The main conclusion from these experiments is that besides the rotation of the spiral wave vector from one spiral domain to another (so called zigzag structure) half-skyrmions usually also appear and may serve as seeds of the skyrmion phase: the cuts of the spiral state in the form of two merons plausibly occurs near the domain boundaries facilitated by their mutual attraction. The first-order phase transition that takes place following this scenario was observed even in the very first experiments in thin-film helimagnets [26,27]. Eventually, such a process of meron formation [25,41] and condensation culminates in the hexagonal arrangement of closely packed skyrmions within the skyrmion lattice phase.

Lorentz transmission electron microscopy investigations of a FeGe wedge-shaped sample Ref. [36] provide additional hints on the most energetically favorable nucleation mechanism of skyrmions. This work reveals domains of coexisting phases—skyrmion clusters and spirals with in-plane and out-of-plane orientations of their wave vectors—with nontrivial domain boundaries between them. Skyrmions were nucleated at the thinner edge of the wedge rather than by pairs of merons generated by spirals. However, domain boundaries between helical domains were observed only above a certain given thickness of the film.

B. Horizontal and vertical skyrmions in chiral liquid crystals

Horizontal skyrmions, which appear within the DWs as shown in Fig. 5, have not been observed experimentally in chiral magnets yet. However, they have been for a long time known in the physics of chiral liquid crystals (CLC) under the name "Lehmann clusters" [42,43]. Indeed, energy contributions phenomenologically analogous to the DMI (3) also arise in chiral liquid crystals [44,45] and are rooted in the acentric shape of the underlying molecules. DMI-like energy terms are responsible for a surprisingly large diversity of naturally occurring and laser-generated topologically nontrivial solitons (including skyrmions) [17,46,47]. In fact, studies of different topological objects with much more sophisticated insight into their 3D structure were gaining momentum in CLCs [17,46,47] well before magnetic skyrmions started attracting a great deal of attention in chiral magnetism. Nowadays CLCs are considered to be highly accessible model systems [43] for probing the behavior and topology of various three-dimensional (3D) knotted structures even with singular field configurations like torons [16,48]. In particular, the discovery and direct visualization of skyrmion clusters with mutually orthogonal orientations of constituent isolated skyrmions [like those depicted in Figs. 3(c) and 5(a)] were reported recently in thin layers of chiral liquid crystals with strong homeotropic anchoring at both surfaces [34]. Such a "horizontal" skyrmion variety remains metastable in the whole field range and develops a weak attractive interaction. Although horizontal skyrmions of this type do not form a lattice, they may couple to vertical skyrmions within the conical domain and additionally tie spiral domains together.

C. Domain-wall-related magnetism in bulk helimagnets

In bulk chiral magnets, domain-wall-related magnetism can be inferred only indirectly. This is the case, e.g., for the polar helimagnet GaV_4Se_8, which manifests a sharp and distinct anomaly in the magnetic susceptibility and the magnetic torque that has been attributed to a transformation of distinct magnetic textures confined to polar domain walls [49]. This geometrical confinement was shown to substantially increase the thermal stability range of magnetic skyrmions, which also survive for quite large angles of an oblique magnetic field. The emergence of these DW-confined magnetic states was tentatively explained as being driven by the mismatch of different spin spirals, hosted by the adjacent structural domains. The results of the present manuscript thus may help to shed light on the fine structure of these domain boundaries. In this respect, the types of the DWs are not restricted to those depicted in Fig. 4 with in-plane orientation of wave vectors. One may envision also horizontal Neel-like half-skyrmions for the horizontal DW orientation.

Lacunar spinels, such as GaV_4S_8, GaV_4Se_8, and $GaMo_4S_8$, were the first material family found to host a Neel-type skyrmion lattice state, which, in the absence of the conical phase, occupies a wide area at the field-temperature phase diagram [22]. While these materials have a cubic structure at high temperatures, many of them transform to a rhombohedral state upon a Jahn-Teller transition what leads to anisotropy axes along $\langle 111 \rangle$ and wave vectors along $\langle 110 \rangle$ directions.

Thus, such an environment with mesoscale polar domains creates prerequisites for the considered DW magnetism.

The experimental findings in a bulk cubic helimagnet Cu_2OSeO_3 [14,50] (Sec. II) also imply the existence of all possible domain boundaries between different spiral states considered theoretically in the present manuscript. Although in an applied magnetic field, only the conical phase represents the most energetically favorable state, the other metastable spirals flip along the field only at the critical field H_{C1} and hence preserve the DW-related topology. Interestingly, in the experiments of Ref. [14], metastable spiral domains reappeared again after decreasing the field from the saturation value. In Ref. [50], however, only the conical phase remains in this case, which excludes the skyrmion nucleation mechanism due to these metastable spiral states. Moreover, it was shown that the region of skyrmion stability is located for much higher magnetic fields than H_{C1} [50]. Therefore, although the domain boundaries between spiral domains host all varieties of skyrmions with half-topological charges, they presumably do not give rise to an extended skyrmion cluster (or skyrmion lattice). The reason might be the following: In reality, domains of metastable spirals are "floating" [schematics in Fig. 1(c)] within the conical phase and thus develop an energetically costly domain boundary with it (in some cases, in the form of vortices). Therefore, the transition field, which in an ideal case of extended helical and SkL phases (i.e., without any domain walls with respect to other phases) corresponds to the line F-G at the phase diagram [Fig. 2(a)], will be larger, if at all achieved. Therefore, such a mechanism is presumably overshadowed by the skyrmion nucleation from domain boundaries between domains of the oblique spirals (Fig. 6), which were reported to directly relate to skyrmion nucleation [14,50]. These culminate also in a pronounced hysteresis of skyrmion stability region for increasing and decreasing magnetic fields, which can be explained by the fact that the larger oblique angle of a spiral state would readily facilitate skyrmion formation.

VII. CONCLUSIONS

In conclusion, we theoretically investigated the internal structure of topological domain boundaries formed between differently oriented helical domains in a bulk helimagnet with additional cubic and exchange anisotropies (1). Such helical domains naturally coexist due to a subtle balance between the Zeeman and anisotropy energies below the critical field H_{C1} and/or the Curie temperature T_C as observed in numerous experiments on B20 helimagnets. Alongside with the charge-free boundaries, the walls may gain a finite topological charge facilitated by the DW's chiral microstructure in the form of half-skyrmions. Depending on the orientation of a DW with respect to the field—DWs are in general oblique and acquire vertical or horizontal projections as limiting cases—interior half-skyrmions run either along or perpendicular to the field. Such nuclei of "full" skyrmions may lead to thermodynamically stable low temperature skyrmions as recently observed in Cu_2OSeO_3. Alternatively, they are responsible for topological anomalies observed experimentally in a variety of chiral magnets. Moreover, the chains of half-skyrmions lead to an efficient coupling to spin currents and thus provide an effective tool to zip and unzip helical domains. We also applied the theoretical results to analyze recent experimental data in chiral magnets and liquid crystals. Together with our earlier findings, the present results provide a consistent picture of the effects generated by the cubic and exchange anisotropy in chiral helimagnets.

ACKNOWLEDGMENTS

The authors are grateful to Ivan Smalyukh and Maxim Mostovoy for useful discussions. A.O.L. thanks U. Nitzsche for technical assistance and acknowledges JSPS Grant-in-Aid (C) No. 21K03406. C.P. acknowledges financial support from the Vrije FOM-programma "Skyrmionics."

[1] A. N. Bogdanov and D. A. Yablonsky, Theormodynamically stable vortices in magnetically ordered crystals. Mixed state of magnetics, Zh. Eksp. Teor. Fiz. **95**, 178 (1989) [Sov. Phys. JETP **68**, 101 (1989)].

[2] A. Bogdanov and A. Hubert, Thermodynamically stable magnetic vortex states in magnetic crystals, J. Magn. Magn. Mater. **138**, 255 (1994); The stability of vortex-like structures in uniaxial ferromagnets, **195**, 182 (1999).

[3] S. Mühlbauer *et al.*, Skyrmion lattice in a chiral magnet, Science **323**, 915 (2009).

[4] H. Wilhelm, M. Baenitz, M. Schmidt, U. K. Rossler, A. A. Leonov, and A. N. Bogdanov, Precursor Phenomena at the Magnetic Ordering of the Cubic Helimagnet FeGe, Phys. Rev. Lett. **107**, 127203 (2011).

[5] S. Seki *et al.*, Observation of skyrmions in a multiferroic material, Science **336**, 198 (2012).

[6] H. Wilhelm *et al.*, Confinement of chiral magnetic modulations in the precursor region of FeGe, J. Phys.: Condens. Matter **24**, 294204 (2012).

[7] U. K. Rößler *et al.*, Skyrmionic textures in chiral magnets, J. Phys.: Conf. Ser. **200**, 022029 (2010).

[8] A. O. Leonov and A. N. Bogdanov, Crossover of skyrmion and helical modulations in noncentrosymmetric ferromagnets, New J. Phys. **20**, 043017 (2018).

[9] P. G. de Gennes, in *Fluctuations, Instabilities, and Phase Transitions*, edited by T. Riste, NATO ASI Ser. B (Plenum, New York, 1975), vol. 2.

[10] U. K. Rößler *et al.*, Spontaneous skyrmion ground states in magnetic metals, Nature **442**, 797 (2006).

[11] O. Janson *et al.*, The quantum origins of skyrmions and half-skyrmions in Cu_2OSeO_3, Nat. Commun. **5**, 5376 (2014).

[12] A. O. Leonov, C. Pappas, and I. Kezsmarki, Field and anisotropy driven transformations of spin spirals in cubic skyrmion hosts, Phys. Rev. Res. **2**, 043386 (2020).

[13] A. Chacon *et al.*, Observation of two independent skyrmion phases in a chiral magnetic material, Nat. Phys. **14**, 936 (2018).

[14] L. J. Bannenberg *et al.*, Multiple low-temperature skyrmionic states in a bulk chiral magnet, npj Quantum Mater. **4**, 11 (2019).

[15] F. Qian *et al.*, New magnetic phase of the chiral skyrmion material $Cu_2OSeO_3$7, Sci. Adv. **4**, eaat7323 (2018).

[16] A. O. Leonov and K. Inoue, Homogeneous and heterogeneous nucleation of skyrmions in thin layers of cubic helimagnets, Phys. Rev. B **98**, 054404 (2018).

[17] P. J. Ackerman and I. I. Smalyukh, Diversity of Knot Solitons in Liquid Crystals Manifested by Linking of Preimages in Torons and Hopfions, Phys. Rev. X **7**, 011006 (2017).

[18] I. E. Dzyaloshinskii, Theory of helicoidal structures in antiferromagnets. I. Nonmetals, J. Sov. Phys. JETP-USSR **19**, 960 (1964); The theory of helicoidal structures in antiferromagnets. II. Metals, **20**, 223 (1965); Theory of helicoidal structures in antiferromagnets. III, **20**, 665 (1965).

[19] P. Bak and M. H. Jensen, Theory of helical magnetic structures and phase transitions in MnSi and FeGe, J. Phys. C: Solid State Phys. **13**, L881 (1980).

[20] A. O. Leonov, C. Pappas, and I. I. Smalyukh, Field-driven metamorphoses of isolated skyrmions within the conical state of cubic helimagnets, Phys. Rev. B **104**, 064432 (2021).

[21] A. O. Leonov, Twisted, localized, and modulated states described in the phenomenological theory of chiral and nanoscale ferromagnets, Ph.D. thesis, Technical University of Dresden, 2012.

[22] I. Kézsmárki *et al.*, Neel-type skyrmion lattice with confined orientation in the polar magnetic semiconductor GaV_4S_8, Nat. Mater. **14**, 1116 (2015).

[23] A. Butykai *et al.*, Characteristics of ferroelectric-ferroelastic domains in Neel-type skyrmion host GaV_4S_8, Sci. Rep. **7**, 44663 (2017).

[24] T. Kurumaji, T. Nakajima, V. Ukleev, A. Feoktystov, T. H. Arima, K. Kakurai, and Y. Tokura, Neel-Type Skyrmion Lattice in the Tetragonal Polar Magnet $VOSe_2O_5$, Phys. Rev. Lett. **119**, 237201 (2017).

[25] J. Müller, J. Rajeswari, P. Huang, Y. Murooka, H. M. Ronnow, F. Carbone, and A. Rosch, Magnetic Skyrmions and Skyrmion Clusters in the Helical Phase of Cu_2OSeO_3, Phys. Rev. Lett. **119**, 137201 (2017).

[26] X. Z. Yu *et al.*, Real-space observation of a two-dimensional skyrmion crystal, Nature **465**, 901 (2010).

[27] X. Z. Yu *et al.*, Near room-temperature formation of a skyrmion crystal in thin-films of the helimagnet FeGe, Nat. Mater. **10**, 106 (2011).

[28] J. C. Loudon, A. O. Leonov, A. N. Bogdanov, M. C. Hatnean, and G. Balakrishnan, Direct observation of attractive skyrmions and skyrmion clusters in the cubic helimagnet Cu_2OSeO_3, Phys. Rev. B **97**, 134403 (2018).

[29] O. Portmann, A. Vaterlaus, and D. Pescia, An inverse transition of magnetic domain patterns in ultrathin films, Nature **422**, 701 (2003).

[30] Y.-T. Shao, S. Das, Z. Hong, R. Xu, S. Chandrika, F. Gomez-Ortiz, P. Garcia-Fernandez, L.-Q. Chen, H. Y. Hwang, J. Junquera, L. W. Martin, R. Ramesh, and D. A. Muller, Emergent chirality in a polar meron to skyrmion phase transition, arxiv:2101.04545 (2021).

[31] A. O. Leonov *et al.*, Three-dimensional chiral skyrmions with attractive interparticle interactions, J. Phys.: Condens. Matter **28**, 35LT01 (2016).

[32] A. O. Leonov *et al.*, Spintronics via nonaxisymmetric skyrmions, Appl. Phys. Lett. **109**, 172404 (2016).

[33] P. Schoenherr *et al.*, Topological domain walls in helimagnets, Nat. Phys. **14**, 465 (2018).

[34] H. R.O. Sohn, S. M. Vlasov, V. M. Uzdin, A. O. Leonov, and I. I. Smalyukh, Real-space observation of skyrmion clusters with mutually orthogonal skyrmion tubes, Phys. Rev. B **100**, 104401 (2019).

[35] F. Li, T. Nattermann, and V. L. Pokrovsky, Vortex Domain Walls in Helical Magnets, Phys. Rev. Lett. **108**, 107203 (2012)

[36] A. O. Leonov, Y. Togawa, T. L. Monchesky, A. N. Bogdanov, J. Kishine, Y. Kousaka, M. Miyagawa, T. Koyama, J. Akimitsu, T. Koyama, K. Harada, S. Mori, D. McGrouther, R. Lamb, M. Krajnak, S. McVitie, R. L. Stamps, and K. Inoue, Chiral Surface Twists and Skyrmion Stability in Nanolayers of Cubic Helimagnets, Phys. Rev. Lett. **117**, 087202 (2016).

[37] F. N. Rybakov, A. B. Borisov, and A. N. Bogdanov, Three-dimensional skyrmion states in thin films of cubic helimagnets, Phys. Rev. B **87**, 094424 (2013).

[38] H. Du *et al.*, Interaction of Individual Skyrmions in a Nanostructured Cubic Chiral Magnet, Phys. Rev. Lett. **120**, 197203 (2018).

[39] D. Capic *et al.*, Skyrmion-skyrmion interaction in a magnetic film, J. Phys.: Condens. Matter **32**, 415803 (2020).

[40] M. Uchida *et al.*, Real-space observation of helical spin order, Science **311**, 359 (2006).

[41] M. Ezawa, Compact merons and skyrmions in thin chiral magnetic films, Phys. Rev. B **83**, 100408 (2011).

[42] S. D. Hudson and E. L. Thomas, Disclination interaction in an applied field: Stabilization of the Lehmann cluster, Phys. Rev. A **44**, 8128 (1991).

[43] I. I. Smalyukh, Review: Knots and other new topological effects in liquid crystals and colloids, Rep. Prog. Phys. **83**, 106601 (2020).

[44] P. Oswald and P. Pieranski, *Nematic and Cholesteric Liquid Crystals: Concepts and Physical Properties Illustrated by Experiments* (CRC Press, Boca Raton, FL, 2005).

[45] M. Kleman and O. D. Lavrentovich, *Soft Matter Physics: An Introduction* (Springer-Vertag, New York, NY, 2003).

[46] I. I. Smalyukh *et al.*, Three-dimensional structure and multistable optical switching of triple-twisted particle-like excitations in anisotropic fluids, Nat. Mater. **9**, 139 (2010).

[47] P. J. Ackerman and I. I. Smalyukh, Static three-dimensional topological solitons in fluid chiral ferromagnets and colloids, Nat. Mater. **16**, 426 (2017).

[48] J.-S. B. Tai, I. I. Smalyukh, Surface anchoring as a control parameter for stabilizing torons, skyrmions, twisted walls, fingers, and their hybrids in chiral nematics, Phys. Rev. E **101**, 042702 (2020).

[49] K. Geirhos *et al.*, Macroscopic manifestation of domain-wall magnetism and mag-netoelectric effect in a Neel-type skyrmion host, npj Quantum Mater. **5**, 44 (2020).

[50] M. Halder *et al.*, Thermodynamic evidence of a second skyrmion lattice phase and tilted conical phase in Cu_2OSeO_3, Phys. Rev. B **98**, 144429 (2018).